

Theory of the Antiferromagnetism of Chromium

I. E. DZIALOSHINSKIĬ AND E. I. KATS

L. D. Landau Institute of Theoretical Physics, USSR Academy of Sciences

Submitted July 29, 1971

Zh. Eksp. Teor. Fiz. 62, 1104–1117 (March, 1972)

It is pointed out that the Hartree-Fock approximation previously used to explain the antiferromagnetism of chromium is inapplicable to this problem. Because of the mathematical complexity of the problem, this fact is demonstrated for a crude model of a metal whose Fermi surface contains two almost plane sections. Numerical solution of the appropriate equations shows that in the case of effective repulsion, there actually occurs in such a system a transition to an antiferromagnetic state. Also investigated are other types of transition that are possible in such a system.

1. INTRODUCTION

THERE is at present a voluminous literature devoted to the investigation of magnetism in a system of collective electrons (see, for example, the monograph of Herring^[1]). Of especial interest are the very peculiar magnetic properties of chromium and some of its alloys. The reason is that in such compounds there is observed experimentally a transition to a state with a "spin density wave" (see the bibliography in^[1]; references on some recent researches will be given in the text of this article). Such a model of antiferromagnetism was first proposed by Overhauser^[2]. Later investigation, however, showed that a spin density wave cannot exist in ordinary metals with an almost spherical Fermi surface. A calculation also made by Overhauser for the one-dimensional case, in the Hartree-Fock approximation, cannot be regarded as a criterion for the existence of such a state, since the Hartree-Fock approximation is inapplicable in the one-dimensional case. Furthermore, by using a result of a paper by Bychkov, Gor'kov, and one of the authors^[3], it is easy to show that an antiferromagnetic spin density wave can in general not occur in a purely one-dimensional case, since the equation for the antiferromagnetic self-energy part (gap) has only a zero solution (see Appendix I). This agrees also with a theorem established by Hohenberg^[4] on the absence in the one-dimensional case, at all finite temperatures, of anomalous pairings. Nevertheless, as has already been mentioned above, it has been shown that such a transition really occurs in chromium and some of its alloys. This is due to the special form of the Fermi surface of chromium; it has symmetrically located plane sections. Here, therefore, there can be fulfillment of the "one-dimensional" condition necessary for existence of a spin density wave; yet at the same time the general objections with regard to the impossibility of antiferromagnetism in a one-dimensional system disappear.

The first theoretical investigation of the problem of the formation of a spin density wave in chromium was made by Lomer (see^[1]); more detailed calculations were recently made by Kimball and Falicov^[5]. In all these papers, however, the Hartree-Fock approximation was used. In the language of diagram technique, this approximation corresponds to summation of a sequence of ladder diagrams for electron-hole pairings

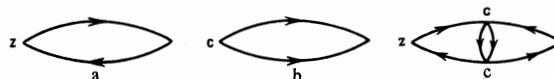


FIG. 1

with transfer of momentum $2p_0$; p_0 is the Fermi momentum on a plane section (see Fig. 1a). But exactly the same contribution to the vertex function is made by diagrams that take account of rescattering of electrons on each other with small total momentum (Fig. 1b). This also shows the inapplicability of the Hartree-Fock approximation in this problem, because in it terms of the same order are omitted.

In the present paper, a systematic calculation is made with logarithmic accuracy to within all "dangerous" diagrams of perturbation theory, for a simplified model of chromium-like compounds. The second section of the paper is devoted to the selection of this model and to a description of the real Fermi surface of chromium. In the third section, the system of equations for the complete vertex part is investigated; its singularities determine also the character of the state of the system. Although the solution of these equations can be found only numerically, nevertheless some general properties of the solutions can be analyzed also in analytic form. Other possible transitions (besides the antiferromagnetic) are considered in our model. In addition, singularities of the heat capacity and of the spin susceptibility at the transition point are studied. A critical analysis of the model and some comparisons with experimental data are given.

2. SELECTION OF THE MODEL

In the literature there is no unique opinion about the form of the Fermi surface of chromium^[1]. Available calculations for d-electrons in the strong-coupling approximation agree qualitatively with experiments on magnetoresistance and the Hall effect, but there is not good agreement with the de Haas-van Alphen effect. We note here that in the space-centered lattice of chromium, in the approximation of strong coupling for the s-electrons (that is, without allowance for degeneracy), the Fermi surface would have the form of a cube.

Most authors assume a form for the Fermi surface of the type shown in Fig. 2. The dotted lines represent the hole of the Fermi surface intersections with the

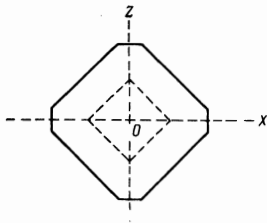


FIG. 2

XZ plane. Of greatest importance to us are the flat sections perpendicular to the X and Z axes. Their presence depends on whether or not, on moving from the point O along the X (or Z) axis, the two- and three-dimensional representations in the group C_{3v} split. Coincidence of these representations does not follow from the symmetry of the lattice and therefore can occur only for an accidental reason. In the case of such coincidence, the flat sections indicated above must disappear. But experiments on the de Haas-van Alphen effect show that in chromium such flat sections apparently exist.

In view of the fact that the detailed form of the Fermi surface of chromium is not known exactly, and also because of mathematical difficulties of the theory for such a Fermi surface, it is helpful to understand the basic regularities in a simple model. We shall consider a metal whose Fermi surface consists of two plane sections of finite extent. Although the presence of supplementary plane sections certainly changes all the equations, there are reasons to suppose that both the character of the singularities and, primarily, the very fact of the existence of a spin density wave remain unchanged (see also Conclusion). An indirect justification of our model is the recently obtained result of Larkin and one of the authors^[6] on the possibility of antiferromagnetic ordering also in a purely one-dimensional case, but with allowance for flipping processes.

3. INSTABILITY OF THE GROUND STATE

We shall now be concerned with a more detailed study of the properties of our model of a metal. The logarithmic accuracy with which we make the calculation is insufficient for investigation of the analytic properties of the vertex part at zero temperature. Therefore we shall use a thermodynamic technique. As has already been mentioned in the Introduction, determination of the vertex function requires summation of all diagrams of the type shown in Figs. 1a and 1b, and of all kinds of insertion of some of them in others (Fig. 1c). These diagrams form a so-called parquet. As usual^[7], the presence of logarithmic terms permits us to separate out the principal diagrams in each order of perturbation theory with respect to the parameter

$$g^2 \max \{ \xi, \eta \}.$$

Here g is some effective interaction, and ξ and η are logarithmic variables (both logarithms of a single order):

$$\xi = \ln \frac{\epsilon_0}{\max \{ T, v |p_1 + p_2|, \omega_1 + \omega_2 \}},$$

$$\eta = \ln \frac{\epsilon_0}{\max \{ T, v |p_3 - p_1 - 2p_0|, \omega_3 - \omega_1 \}}.$$

The cutoff at a characteristic atomic energy ϵ_0 is due to the effectiveness of the interaction only at interatomic distances. The meaning of the momenta and frequencies that occur in the argument of the logarithm is clear from Fig. 3; T is the temperature, v is the Fermi velocity.

In our model, however, there is an important difference from the purely one-dimensional case. It is due to the finiteness of the plane sections of the Fermi surface (the plane sections do not occupy the whole first Brillouin zone). Therefore all the diagrams, besides depending on the logarithmic variables ξ and η , depend also on the transverse momenta, and in non-logarithmic fashion (a logarithmic integration results only when no one of the momenta extends to the edges of the plane sections). For example, the "Cooper" diagram (Fig. 1c) is equal to

$$g^2 v \xi S_c.$$

Here

$$v = \frac{1}{(2\pi)^3} \int \frac{d^3 l}{|v(l)|}$$

is the density of states on the Fermi surface (l here and everywhere hereafter is the transverse momentum); the quantity S_c is proportional to the area of the Fermi surface on which the logarithmic integration is carried out:

$$S_c = \frac{2}{v} \int \frac{d^2 l}{|v(l)| + |v(l-c)|},$$

where $c = l_1 + l_2$ is the total incoming transverse momentum, and the integral is taken only over those values of l for which both l and $l - c$ lie on the plane section of the Fermi surface.

Similarly the "zero-sound" diagram (Fig. 1a) is equal to

$$g_z v \eta S_z,$$

where

$$S_z = \frac{2}{v} \int \frac{d^2 l}{|v(l)| + |v(l-z)|},$$

$z = l_1 - l_3$ is the momentum transfer, and the integral is again extended only over that part of the Fermi surface where both momenta (l and $l - z$) lie on the plane sections. Thus in our model there is a "fast" dependence on the transverse momenta. This fact severely complicates the calculation of the complete vertex in the "parquet" approximation.

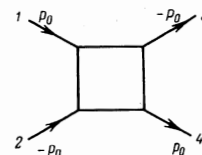


FIG. 3

We choose the bare interaction between the electrons in the following form (Fig. 3):

$$\Gamma_{\alpha\beta\gamma\delta}^{(0)}(p_0, -p_0, -p_0, p_0) = g_1(\delta_{\alpha\gamma}\delta_{\beta\delta} - \delta_{\alpha\delta}\delta_{\beta\gamma}) + g_2\delta_{\alpha\delta}\delta_{\beta\gamma}; \quad (1)$$

here $\alpha, \beta, \gamma,$ and δ are spin indices. Within the conditions

$$|p_1 + p_2| \ll p_0, \quad |p_3 - p_1 - 2p_0| \ll p_0$$

the complete vertex function Γ depends only on the two logarithmic momenta ξ and η and on the transverse momenta l (a vertex reducible in the direction $p_1p_4 \rightarrow p_2p_3$ contains in general no logarithmic integration):

$$\Gamma = \Gamma(l, l_1, l_2, l_3, l; \xi, \eta).$$

Because of conservation of momentum, only three transverse momenta are independent. It is convenient to consider two different sets of variables:

$$\Gamma(l, l', c; \xi) \text{ and } \tilde{\Gamma}(l, l', z; \xi), \quad (2)$$

where $l \equiv l_1, l' \equiv l_3$; because of conservation of momentum,

$$l + l' = c + z. \quad (3)$$

With the notation (2), it has already been taken into account that, as usual^[7] in the parquet approximation, when all the momenta involved are of a single order, the vertex function depends only on a single logarithmic momentum.

The system of parquet equations is recorded most simply by seeking a solution in the following form with respect to the spin indices (analogous to (1)):

$$\Gamma_{\alpha\beta\gamma\delta} = \Gamma_1(\delta_{\alpha\gamma}\delta_{\beta\delta} - \delta_{\alpha\delta}\delta_{\beta\gamma}) + \Gamma_2\delta_{\alpha\delta}\delta_{\beta\gamma}. \quad (4)$$

Here it is convenient to break up the complete vertex into reducible parts (for the time being we omit the spin variables):

$$\Gamma = g + C + Z; \quad (5)$$

C —the so-called Cooper block—is the aggregate of diagrams reducible in the direction $p_1p_2 \rightarrow p_3p_4$; Z is the “zero-sound block”, reducible with respect to the direction $p_1p_3 \rightarrow p_2p_4$. If we now choose the spin structure of the blocks in the form (4), we get the following system of equations:

$$C_{3,2}(l, l', c, \xi) = g_{3,2} + \int_0^1 d\lambda \int dS_c'' \Gamma_{3,2}(l, l'', c; \lambda) \Gamma_{3,2}(l'', l', c; \lambda), \quad (6)$$

$$Z_{\pm}(l, l', z; \xi) = g_{\pm} \mp \int_0^1 d\lambda \int dS_c'' \tilde{\Gamma}_{\pm}(l, l'', z; \lambda) \tilde{\Gamma}_{\pm}(l'', l', z; \lambda),$$

where $\Gamma_3 = -2\Gamma_1 + \Gamma_2$ (and analogously C_3), $\Gamma_{\pm} = \Gamma_1 \pm \Gamma_2$ (and analogously Z_{\pm});

$$dS_c'' = \frac{2}{v} \frac{d^2l''}{|v(l)| + |v(l-z)|},$$

$$dS_c'' = \frac{2}{v} \frac{d^2l''}{|v(l)| + |v(l-c)|}.$$

Furthermore, in the derivation of (6) it has been taken into account that for $\xi > \eta$ the zero-sound block depends only on the one largest logarithmic momentum, and similarly, for $\xi < \eta$, the Cooper block.

If equations (6) did not contain integrations with re-

spect to the transverse momenta, they would reduce in the usual way^[7] to differential equations, and their solutions would have the following form:

$$\Gamma \sim 1 / (\xi - \xi_0), \quad (7)$$

where $\xi_0 = g \ln(\epsilon_0/T_C)$ is a fixed pole, determining the transition temperature T_C . (Here and everywhere hereafter, the constants g in the appropriate combination are included in the definition of ξ .) Equations (6) are also satisfied by solution with a fixed pole, but with a residue dependent on l and l' ; because of the non-logarithmic integrals, however, there are also other possibilities. As for the parquet solutions (7), as has already been indicated, they do not lead to antiferromagnetism, and therefore we shall for the time being disregard them.

It is easily recognized that there remain two types of solution of equations (6) with singularities in the form of “mobile” poles. For this purpose it is necessary to substitute in equations (6)

$$C_{3,2} = \gamma_{3,2}(l, l', c) / [\xi - \xi_{3,2}(c)] \quad (8a)$$

or

$$Z_{\pm} = \tilde{\gamma}_{\pm}(l, l', z) / [\xi - \xi_{\pm}(z)], \quad (8b)$$

where $\gamma_{3,2}$ and $\tilde{\gamma}_{\pm}$ no longer have singularities. In case (8a) there is a pole in the Cooper channel, dependent on the total momentum c . If we substitute (8a) in the zero-sound channel, then because of the integration with respect to c (in this channel z is conserved) we still obtain a cut. Analogously, (8b) corresponds to a pole in the zero-sound channel, which gives a cut on integration with respect to the momentum transfer z in the Cooper channel. Substitution of (8) in (6) gives the equations for the residues at the poles:

$$\gamma_{3,2}(l, l', c) = - \int dS_c'' \gamma_{3,2}(l, l'', c) \gamma_{3,2}(l'', l', c), \quad (9)$$

$$\tilde{\gamma}_{\pm}(l, l', z) = \pm \int dS_c'' \tilde{\gamma}_{\pm}(l, l'', z) \tilde{\gamma}_{\pm}(l'', l', z). \quad (10)$$

The presence of different poles in vertex parts of different spin structure, and also the appearance of different poles in different channels (Cooper and zero-sound), lead to the appearance of simple poles in the generalized susceptibility. But the appearance of a pole in the generalized susceptibility corresponds to a definite type of instability (a phase transition). This problem will be considered in more detail in section 4. But now we shall simply enumerate the instabilities that are possible in our system. A pole in the zero-sound channel, at \tilde{Z}_{-} , corresponds to an antiferromagnetic

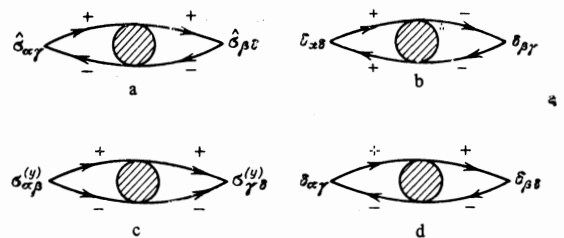


FIG. 4



FIG. 5

transition (the generalized susceptibility is represented in Fig. 4a), a pole at \bar{Z}_+ to a dielectric transition (instability in the distribution of electron density with respect to a doubling of the period (Fig. 4b)); a pole in the Cooper channel at C_3 corresponds to a superconductive pairing with zero spin (Fig. 4c), at C_2 to a superconductive pairing with spin unity (Fig. 4d).

We consider as an example the antiferromagnetic transition. We calculate the behavior of the appropriate susceptibility near the pole. For this purpose, it is necessary to write the equation for the polarization operator (Fig. 5). For example,

$$\Pi_-(\xi, l, z) = \int_0^{\xi} d\lambda T_-(\lambda, l', z) dS_l''; \quad (11)$$

T is the complete triple vertex. From Fig. 6 follows obviously the equation for the triple vertex (differentiated, for convenience, with respect to the logarithmic momentum):

$$\frac{dT_-}{d\xi} = \int dS_l \Gamma_- T_-; \quad (12)$$

On substituting from (8b), we get

$$\frac{dT_-}{d\xi} = \frac{1}{\xi - \xi_0} \int dS_{l'} \Gamma_-(l, l') T_-(l'). \quad (13)$$

The solution of (13) has the form

$$T_- = f(l)/(\xi - \xi_0), \quad (14)$$

where the function f satisfies the equation

$$f(l) = - \int dS_{l'} \Gamma_-(l, l') f(l').$$

From (14) and (11) the polarization operator is

$$\Pi_-(\xi, z) = \frac{1}{\xi_0 - \xi} \int dS_l f^2. \quad (15)$$

The other vertices can be investigated similarly.

Different types of solution of equations (6) correspond to different types of phase transition that are possible in the system under consideration. For determination of the true character of the ground state at $T < T_c$, it is necessary to effect a joining together of the solutions (8) with perturbation theory. To do this in analytic form does not appear possible in view of the mathematical difficulties. Therefore a numerical solution of the system of equations (6) was found; for convenience in the calculation, the transverse momentum l'' , with respect to which the integration occurs in the equations, was considered one-dimensional. This limitation in the present case has no importance in principle, since in the parquet approximation there are no fluctuations for which the dimensionality of the space is important. The only important fact is the occurrence of mobile poles in the presence of nonlogarithmic variables.

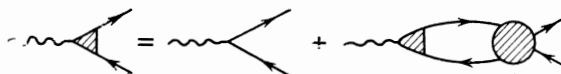


FIG. 6

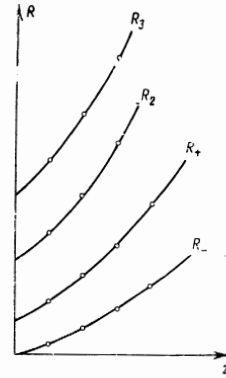


FIG. 7

Vertex	Radius of convergence	
	6th iteration	7th iteration
Γ_-	6.490	6.482
Γ_+	6.712	6.620
Γ_2	6.901	6.807
Γ_3	7.145	7.002

A solution was sought in the form of an expansion as a series in ξ (a connection with perturbation theory). Then the position of the nearest singularity was identified as the radius of convergence of this series. The radius of convergence R was calculated as the limit of the ratio of coefficients. The results for the nearest singularities of the various vertices, after the sixth and seventh integrations, are shown in the table (the spacing $h = 0.02$). The position of the singularities in the vertices as it depends on the transverse momentum is shown in Fig. 7. The following facts require mention: a) the integration behaves monotonically; b) with increase of the number of integrations, the trajectory of the pole becomes more sloping; c) the trajectories of the singularities of different vertices do not intersect; d) the smallest value of the singularity, for all the vertices, occurs at the center of the plane section; e) the smallest radius of convergence is that for the vertex Γ_- ; f) the trajectory of the singularity can be described approximately in the following form:

$$R_- = az^2, \quad (16)$$

where the coefficient $a = 0.251$.

From all that has been said, it may be concluded that in our model there actually occurs an antiferromagnetic transition, in which the spin density has a periodic distribution with the doubled interatomic period $2p_0$. This follows from the fact that a singularity appears first in the antiferromagnetic vertex^[3] (see also the Conclusion).

As has already been mentioned above, besides the singularities that have been found, with mobile poles, in equations (6) there can also occur a singularity of the usual parquet type. The nature of the singularities that are then obtained in the susceptibilities is demonstrated in Appendix II.

To conclude this section, we shall investigate the range of applicability of our solutions. The corrections to the pole terms (8) from the parquet diagrams are

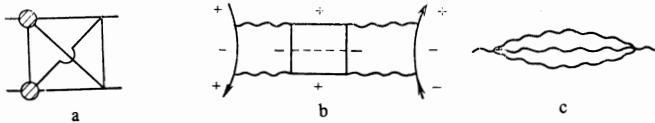


FIG. 8

determined by integrals over the transverse momenta, and they are small: $\sim g \ln(\Gamma/g)$. As regards the contributions of the nonparquet diagrams (for example, the so-called envelope of Fig. 8a), in the range where the logarithmic approximation is applicable, that is, not too close to the transition point (for more details see below), they are also small. This is connected with the integrations over the transverse momenta, which affect the mobile poles in the vertices but not the one-dimensional Green functions. But in the nonlogarithmic vicinity of a pole, where the corresponding bare vertices must take the "normal" three-dimensional form

$$\Gamma = \frac{g}{T - T_c + k_z^2 + ak_\perp^2}, \tag{17}$$

all the diagrams begin to play an important role. This can be conveniently understood directly from the graphs (Fig. 8b and c). For example, diagram 8b corresponds to corrections to the nonsingular vertices in our problem (as is symbolized by the dotted line). The correction to the singular vertex (17) (symbolized by the wavy line) is given in graph 8c. A simple calculation with the aid of (17) gives, for example, for Fig. 8b an expression $\sim (T - T_c)^{-1}$. This pole singularity will then be reproduced both in the envelope and in the other diagrams. The nature of the singularities in this region can be determined, for example, from the theory of similitude (scaling). We will not discuss this here but will only mention that the scaling region is determined, in analogy to the theory of superconductivity, by the ratio $(T_c/\epsilon_F)^\gamma$. In our approximation, because of the exponential smallness of the transition temperature, this region of strong coupling is small. The constant γ is determined by the nature of the diagrams (of the type shown in Fig. 8c) that determine the self-energy part of the fluctuations Σ . If $\Sigma \sim k^{-3/2}$, $\gamma = 4$. In the general case, the power γ is determined by two scaling indices, α and β ,

$$\Sigma = k_z^\alpha f(k_\perp^2/k_z^\beta).$$

Here it follows from the equation for Σ that

$$2\alpha = 2\beta + 1, \quad \gamma = 2\alpha + \beta.$$

Hereafter we shall not be further concerned with this region.

4.. SUSCEPTIBILITY AND OTHER TYPES OF TRANSITION

All the possible phase transitions in our model are determined by the singularities of the various vertex parts or of the generalized susceptibilities connected



FIG. 9



FIG. 10



FIG. 11

with them. The corresponding quantities are represented in Fig. 4. The case, already investigated above, of a transition to a state with a spin density wave is connected with singularities in the vertex Γ_- . This is easily seen from the diagram of Fig. 4a, which gives the antiferromagnetic generalized susceptibility. We shall now calculate the correction, according to perturbation theory, to the ordinary spin susceptibility and the heat capacity (the diagrams of Figs. 9 and 10). The analytic expression for the diagram of Fig. 9 has the following form:

$$\sigma_{\alpha\gamma} \sigma_{\beta\delta} [\Gamma_1 (\delta_{\alpha\gamma} \delta_{\beta\delta} - \delta_{\alpha\delta} \delta_{\beta\gamma}) + \Gamma_2 \delta_{\alpha\delta} \delta_{\beta\gamma}], \tag{18}$$

where σ^i are the Pauli matrices. From expression (18) it follows that

$$\chi = \int d^2l d^2z \tilde{\Gamma}_1(l, l, z; \xi). \tag{19}$$

On differentiating the equality (19) with respect to the logarithmic momentum and using the parquet equations (6), we get

$$\frac{d\chi}{d\xi} = \int d^2l d^2l' d^2z \tilde{\Gamma}_1(l, l', z; \xi). \tag{20}$$

The expression (20) corresponds to the diagram shown in Fig. 11. But since

$$\Gamma_1 = [\xi_0 - \xi + az^2]^{-1},$$

it follows from (20) that

$$d\chi/d\xi \sim 1/(\xi_0 - \xi)$$

or

$$\chi \sim \ln(\xi_0 - \xi) = \ln[(T - T_c)/T_c]. \tag{21}$$

Thus there is a logarithmic addition ($\sim g^2$) to the susceptibility. (The transition temperature T_c is determined from the condition $\xi_0 = \xi$.) A behavior of this type is not inconsistent with the experimental data^[8] and of course cannot be obtained in the self-consistent field approximation^[5].

Similarly, it is easy to calculate the heat capacity for $T > T_c$. Here it is necessary to take into account that the singular parts of all thermodynamic quantities (such as, for example, the free energy) connected with the antiferromagnetic transition can be considered to depend only on the difference $T - T_c$. Therefore derivatives of thermodynamic quantities with respect to the temperature T can be replaced by derivatives with respect to T_c . Furthermore, by use of the condition $\xi(T_c) = \xi_0$, it is possible to reduce everything to differentiation with respect to ξ_0 . Thus we have

$$C \sim \frac{\partial^2 F}{\partial T^2} \sim \left(\frac{d\mu}{dT_c} \right)^2 \frac{\partial^2 F}{\partial \mu^2} \sim \frac{\partial^2 F}{\partial \xi_0^2} \sim \ln(\xi_0 - \xi) \tag{22}$$

(here μ is the chemical potential). In writing formula (22), use has been made of the fact that the heat capacity is given by the diagram of Fig. 10, which reduces to an integral from $-\Gamma_1 + 2\Gamma_2 \sim \Gamma_-$.

Depending on the sign and values of the bare interactions, other vertex functions or generalized suscep-

tibilities, also, may have singularities. Thus, for example, for $g_1 < 0$ and $g_2 = 0$ there is a nearest singularity with a pole of the mobile type at the vertex Γ_3 (Fig. 4c). This singularity in the corresponding susceptibility gives a transition to the superconducting state in our system; pairs form in the singlet state. The situation here is analogous to the antiferromagnetic in the sense that there is a mobile pole singularity, but from its minimum value goes a cut considerably less strongly dependent on the momenta.

For a phase transition determined by a stationary pole, there must occur simultaneously with superconductivity also a doubling of the period^[3]. In the case when the nearest pole is at the vertex Γ_+ (Fig. 4b), the corresponding transition has dielectric character, and there is a doubling of the period. Finally, if the nearest singularity is at the vertex Γ_2 (Fig. 4d), then a superconducting state is obtained, but pairs with zero moment are formed (triplet pairing). This exhausts all the possible transitions in our model. We once more emphasize that all superconducting transitions are due to the presence of attraction, $g_{1,s} < 0$, whereas for magnetic transitions an effective repulsion, $g_{\pm} > 0$, is essential.

We shall lead up to the conclusion of our results. The most important result of our research is the establishment of the very fact of the possibility of an antiferromagnetic transition to a state with a spin density wave, by systematic consideration of a model with plane sections. It has been shown that the transition has a very peculiar character. Our model, despite its rather approximate character, qualitatively describes correctly the substance of the antiferromagnetic transition in chromium-like alloys. Of course the analytically best approximation to the true Fermi surface of chromium would be a model of a metal whose Fermi surface has the form of a cube. Although writing down the parquet equations for a cube presents no difficulties, even a numerical solution of them is very difficult because of the many-dimensional integrations. Even more impossible in the general analysis of the solution in analytic form, carried out in Sec. 3 of the present paper. Leaving the investigation of this problem to a separate article, we shall mention here only that there are considerations that allow us to suppose that the conclusion regarding the presence of a phase transition to a state with a spin density wave remains correct also for a Fermi surface in the form of a cube. One of these considerations was stated in the Introduction; a second is the fact that the trajectories of the poles of different vertex functions in the plane of the bare constants g_1 and g_2 on different faces of the cube never intersect. Therefore, starting from an antiferromagnetic state far from the singularity (which can always occur in the presence of an effective repulsion), we must obtain an antiferromagnetic character for the transition.

Furthermore, the model presented is in reasonable qualitative agreement with experimental data on the dependence of the transition temperature on impurities and pressure^[1]. Although a quantitative comparison is impossible because it requires going beyond the framework of the logarithmic approximation, the general behavior of the transition temperature can be understood

even in our simple model. For example, addition of vanadium impurity to chromium decreases the size of the plane sections of the Fermi surface, and this for some concentration must lead to a disappearance of the transition. This same effect is responsible for the dependence of the period of the structure ($2p_0$) on the impurity concentration.

The authors express their tanks to A. Kh. Rakhmatulinaya for the numerical solution of equations (6).

APPENDIX I

The equation for the antiferromagnetic gap κ in the purely one-dimensional case has the following form (see^[3]):

$$\kappa(\xi) = C_-(\xi) \int_{\xi}^{\xi_{\text{eff}}} \kappa(t) dt + \int_{\xi}^{\xi} C_-(t) \kappa(t) dt. \tag{A.1}$$

Here $\xi_{\text{eff}} = \ln(\epsilon_0/\delta)$, where δ is a quantity of the order of κ , at which the logarithmic integration must be cut off (on the Fermi surface $\delta = 0$). The one-dimensional equation (A.1) has a nonvanishing solution only if the corresponding non-one-dimensional equation has a pole. The corresponding non-one-dimensional equation is obtained by adding to the right side of equation (A.1) the Cooper block $C_-(\xi)$. In this process, there is obtained an equation for Γ_- which, in a purely one-dimensional system, has no poles with respect to ξ , for $\xi > \eta$ ^[3]. This also proves the statement made in the text that $\kappa = 0$.

We mention here that for our model at $T < T_c$ it is possible to write an equation for the gap analogous to (A.1) (the transverse integrations will still enter). From such an equation it is easy to obtain a relation of the type

$$\kappa = T_c f(\xi). \tag{A.2}$$

But to determine the function $f(\xi)$ (even with logarithmic accuracy), it is necessary to know the behavior of the vertices far from the singularity, and this is impossible within the framework of the present research.

APPENDIX II

We investigate the nature of the singularities that occur in the presence of a fixed pole. For this purpose we introduce the quantities

$$c + z = \gamma,$$

Then according to formula (9) of the main text of the article, we have

$$c_{3,2} = - \int dS_c \gamma_{3,2}(l, l'') \gamma_{3,2}(l'' l'). \tag{A.3}$$

$$\tilde{z}_{\pm} = \pm \int dS_c \tilde{\gamma}_{\pm}(l, l'') \tilde{\gamma}_{\pm}(l'' l').$$

Analogously one can obtain

$$2z_2 = \int dS_c \{\tilde{\gamma}_+^2 + \tilde{\gamma}_-^2\}, \quad 2z_1 = \int dS_c \{\tilde{\gamma}_+^2 - \tilde{\gamma}_-^2\} \tag{A.4}$$

or

$$z_2 = \int dS_c \{\tilde{\gamma}_1^2 + \tilde{\gamma}_2^2\}, \quad z_1 = 2 \int dS_c \tilde{\gamma}_1 \tilde{\gamma}_2, \tag{A.5}$$

and also

$$c_1 = 2 \int dS_c \{\gamma_1^2 + \gamma_2 \gamma_2\}, \quad c_2 = - \int dS_c \gamma_2^2. \tag{A.6}$$

From (A.5) and (A.6) follows

$$\begin{aligned}\gamma_2 &= \int dS_z \{\bar{\gamma}_1^2 + \bar{\gamma}_2^2\} - \int dS_c \gamma_2^2, \\ \gamma_1 &= 2 \int dS_c \bar{\gamma}_1^2 - 2 \int dS_c \bar{\gamma}_1 \gamma_2 + 2 \int dS_z \bar{\gamma}_1 \gamma_2.\end{aligned}\quad (\text{A.7})$$

From formulas (A.7) one can write the quantities of interest to us, $\gamma_3, \gamma_2, \bar{\gamma}_{\pm}$:

$$\begin{aligned}\gamma_3 &= - \int dS_c \gamma_2^2 + \frac{1}{2} \int dS_z (\bar{\gamma}_-^2 + \bar{\gamma}_+^2), \\ \bar{\gamma}_+ &= \int dS_z \bar{\gamma}_+^2 - \frac{1}{2} \int dS_c (3\gamma_2^2 - \gamma_3^2), \\ \bar{\gamma}_- &= - \int dS_z \bar{\gamma}_-^2 + \frac{1}{2} \int dS_c (\gamma_2^2 + \gamma_3^2)\end{aligned}\quad (\text{A.8})$$

(γ_2 has already been written in (A.7)).

On making in equations (A.8) and (A.7) the substitution $\mathbf{c} \rightarrow \mathbf{z}$, where $\mathbf{l} + \mathbf{l}' = \mathbf{c} + \mathbf{z}$, it is easy to perceive that the following relations hold:

$$\begin{aligned}\bar{\gamma}_+(l, l', \mathbf{z}) &= -\gamma_3(l, l', \mathbf{z}), \quad \gamma_2(l, l', \mathbf{z}) = \bar{\gamma}_-(l, l', \mathbf{z}), \\ \gamma_3(l, l', \mathbf{c}) &= -\bar{\gamma}_+(l, l', \mathbf{c}).\end{aligned}\quad (\text{A.9})$$

Therefore equations (A.8) can be rewritten in the following form:

$$\begin{aligned}\gamma_3(\mathbf{c}) &= - \int dS_c \gamma_3^2(\mathbf{c}) + \frac{1}{2} \int dS_z [3\gamma_2^2(\mathbf{z}) - \gamma_3^2(\mathbf{z})], \\ \gamma_2(\mathbf{c}) &= - \int dS_c \gamma_2^2(\mathbf{c}) + \frac{1}{2} \int dS_z [\gamma_2^2(\mathbf{z}) + \gamma_3^2(\mathbf{z})]\end{aligned}\quad (\text{A.10})$$

or

$$\begin{aligned}\gamma_3(\mathbf{z}) &= - \int dS_z \gamma_3^2(\mathbf{z}) + \frac{1}{2} \int dS_c [3\gamma_2^2(\mathbf{c}) - \gamma_3^2(\mathbf{c})], \\ \gamma_2(\mathbf{z}) &= - \int dS_z \gamma_2^2(\mathbf{z}) + \frac{1}{2} \int dS_c [\gamma_2^2(\mathbf{c}) + \gamma_3^2(\mathbf{c})].\end{aligned}\quad (\text{A.11})$$

Hence it is possible to deduce that

$$\gamma_2(\mathbf{c}) = -1/2 [\gamma_2(\mathbf{z}) + \gamma_3(\mathbf{z})], \quad \gamma_3(\mathbf{c}) = -1/2 [3\gamma_2(\mathbf{z}) - \gamma_3(\mathbf{z})]. \quad (\text{A.12})$$

Also, inversely,

$$\gamma_2(\mathbf{z}) = -1/2 [\gamma_2(\mathbf{c}) + \gamma_3(\mathbf{c})], \quad \gamma_3(\mathbf{z}) = -1/2 [3\gamma_2(\mathbf{c}) - \gamma_3(\mathbf{c})]. \quad (\text{A.13})$$

It is now possible to write equations (A.8) in their simplest form:

$$\begin{aligned}\gamma_2 &= 4 \int \bar{\gamma}_2^2 dS_c, \quad \gamma_3 = -4/3 \int \bar{\gamma}_3^2 dS_c, \\ \bar{\gamma}_+ &= 4/3 \int \bar{\gamma}_+^2 dS_z, \quad \bar{\gamma}_- = 4 \int \bar{\gamma}_-^2 dS_z.\end{aligned}\quad (\text{A.14})$$

The relations (A.14) allow us easily to write an expres-

sion for the derivative, with respect to the logarithmic momentum, of an arbitrary generalized susceptibility (at the pole). For example, for the susceptibility connected with the vertex γ_3 we have (in analogy to the derivation of formulas (11)–(14) of the text)

$$d\Pi_3/d\xi = \int T_3^2 dS_c, \quad (\text{A.15})$$

where Π_3 is the "polarization" operator and T_3 is the triple vertex:

$$\frac{dT_3}{d\xi} = \int \Gamma_3(l, l') T_3 dS_c = \frac{1}{\xi - \xi_0} \int \gamma_3(l, l') T_3 dS_c.$$

On introducing the notation

$$J = \int \gamma_3(l, l') T_3 dS_c$$

and using (A.14), we have

$$\frac{dJ}{d\xi} = -\frac{3}{4} \frac{1}{\xi - \xi_0} J$$

or

$$J = \frac{f}{(\xi_0 - \xi)^{3/4}}, \quad T_3 = \frac{F}{(\xi_0 - \xi)^{3/4}}. \quad (\text{A.16})$$

Also, finally, from (A.15)

$$\Pi_3 \sim (\xi_0 - \xi)^{-1/2}. \quad (\text{A.17})$$

The generalized susceptibility Π_+ behaves completely analogously. This follows from the equations

$$\frac{d\Pi_+}{d\xi} = \int T_+^2 dS_c, \quad (\text{A.18})$$

$$\frac{dT_+}{d\xi} = -\frac{1}{\xi - \xi_0} \int \bar{\gamma}_+(l, l') T_+ dS_c. \quad (\text{A.19})$$

Also, in accordance with (A.14),

$$\Pi_+ \sim (\xi_0 - \xi)^{-1/2}. \quad (\text{A.20})$$

¹Magnetism (G. T. Rado and H. Suhl, editors), Vol. 4, Academic Press, 1966.

²A. W. Overhauser, Phys. Rev. Lett. **4**, 462 (1960).

³Yu. A. Bychkov, L. P. Gor'kov, and I. E. Dzyaloshinskiĭ, Zh. Eksp. Teor. Fiz. **50**, 738 (1966) [Sov. Phys.-JETP **23**, 489 (1966)].

⁴P. C. Hohenberg, Phys. Rev. **158**, 383 (1967).

⁵J. C. Kimball and L. M. Falicov, Phys. Rev. Lett. **20**, 1164 (1968).

⁶I. E. Dzyaloshinskiĭ and A. I. Larkin, Zh. Eksp. Teor. Fiz. **61**, 791 (1971) [Sov. Phys.-JETP **34**, 422 (1972)].

⁷V. V. Sudakov, Dokl. Akad. Nauk SSSR **111**, 338 (1956) [Sov. Phys.-Dokl. **1**, 662 (1956)]; B. Roulet, G. Gavoret, and P. Nozières, Phys. Rev. **178**, 1072 (1969).

⁸D. Bender and J. Müller, Phys. Kondens. Mater. **10**, 342 (1970).